Dynamic slowing down in dense percolating microemulsions

P. Tartaglia

Dipartimento di Fisica, Università di Roma La Sapienza, Piazzale Aldo Moro 2, I-00185 Roma, Italy

J. Rouch

Centre de Physique Moléculaire Optique et Hertzienne, Université Bordeaux I, 351 Cours de la Libération, 33405 Talence CEDEX, France

S. H. Chen

Department of Nuclear Engineering and Center for Materials Science and Engineering, Massachusetts Institute of Technology, Cambridge, Massachusetts 02139

The dynamic slowing down of the first cumulant and the stretched exponential decay of the droplet density-time correlation function at long time, previously observed for the one-phase sodium-di-2-ethylhexylsulfosuccinate (AOT)–water–decane microemulsion system, are attributed to the approach to a percolation threshold as the volume fraction of the microemulsion is increased at constant temperature. A model for dynamic light scattering, formulated along the line of the scattering from a system of transient polydispersed fractal clusters, quantitatively accounts for all the light-scattering data reported so far and also for some additional results.

I. INTRODUCTION

The structure and dynamics of a three-component ionic microemulsion system, AOT (sodium-di-2-ethylhexylsulfosuccinate)–water–decane, has been extensively studied by neutron and light scattering in the past ten years [1–5]. It has been firmly established that in the vicinity of room temperature, a one-phase microemulsion, called the L_2 phase, occupies a large area of the Gibbs triangle stretching out from the oil corner. Small-angle neutron-scattering experiments showed that throughout the L_2 phase the microemulsion consists of water droplets coated by a monolayer of surfactant molecules, dispersed in a continuum of oil. Assuming that the solution is incompressible, we can calculate the volume fraction of the dispersed phase ϕ as $\phi = \phi_w + \phi_s$, where ϕ_w and ϕ_s are the volume fractions of the water and the surfactant, respectively. When the molar ratio of water to surfactant, $X = [\text{water}]/[\text{surfactant}]$, is kept constant at say 40.8, the water core has an average radius of about 50 Å and the one-phase microemulsion shows a large variety of interesting physical phenomena upon varying the temperature or/and the volume fraction of the dispersed phase. The latter quantity can be adjusted by changing the amount of decane in the sample while keeping X constant. The T-ϕ phase diagram of the system with $X = 40.8$ depicted in Fig. 1 shows a cloud point curve, separating the lower homogeneous microemulsion phase from the upper two-phase microemulsions, extending from $\phi = 0.04$ to 0.40. This cloud point curve, which is also the coexisting curve for the pseudoternary system, has a highly asymmetric shape with a lower consolute point occurring at $\phi_c = 0.098$ and $T_c = 39.960$ °C. The

phase separation line ends abruptly in a cusp at $\phi = 0.40$ and $T = 50$ °C, where it joins to another phase boundary separating the homogeneous microemulsion phase (at lower temperatures) from a lamellar phase L_α (at higher temperatures). In the T-ϕ phase diagram shown in Fig. 1 there is also a percolation line that we determined by electrical conductivity measurements [6]. We show in the inset of Fig. 1 the value of the electrical conductivity as a function of volume fraction, at constant temperatures, which increases by 5 orders of magnitude when crossing the percolation line. The behavior of the electrical conductivity over a large domain of the phase diagram can be explained as follows. Far below the percolation threshold, the conductivity can be well described by the fluctuating charge model of Eicke, Borkovec, and Das-
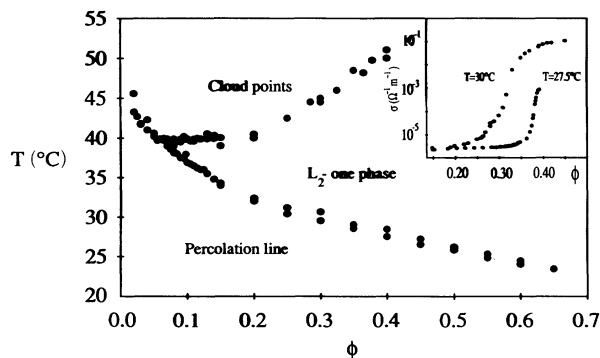

FIG. 1. The phase diagram of the AOT–water–decane microemulsion at $X = 40.8$. The inset shows two typical electrical conductivity curves at percolation.

Gupta [7] for a large interval of volume fractions. In this model, the mechanism of charge transport resulting in conduction is attributed to the Brownian diffusion of charged droplets. Under this mechanism the electrical conductivity can be shown generally to be equal to the mean-square fluctuation of charges of the droplets divided by the Stokes friction coefficient. The droplets acquire charges owing to exchange of monomers between the droplets and the surrounding pool of monomers. The mean-square charge fluctuation has been calculated using a thermodynamic fluctuations theory by Eicke, Borkovec, and Das-Gupta. In this theory the conductivity is proportional to the volume fraction and temperature. Hall [8] has recently improved the calculation of the mean-square charge fluctuation by considering more carefully the monomer-droplet chemical equilibrium. In the resultant theory the conductivity is a nonlinear function of temperature which depends on the maximum number of charges a droplet can acquire. We have been able to analyze the temperature dependence of the conductivity at low volume fractions and concluded, based on the Hall theory, that the maximum charge on a droplet is one electron. As the volume fraction increases beyond 0.10 the charge fluctuation theory fails and the system begins to show electrical percolation behavior. Close to the percolation threshold the increase of the low-frequency conductivity can be described by a power-law divergence with an exponent s' which has the value expected for a dynamic percolation, $s'=1.2\pm0.1$ [9,10]. In this regime it can be conjectured that transient fractal clusters are formed in the dense-microemulsion system so that surfactant molecules (anions) or counterions (cations) can migrate from droplet to droplet within a cluster. The overall shape of the percolation line, which is asymptotically tangential to the spinodal line associated with the cloud point curve, can be accounted for theoretically by using a model of percolation in probability due to Xu and Stell [11]. The model assumes an interdroplet potential consisting of a hard core plus a small but long-ranged attractive Yukawa tail with temperature-dependent parameters [12]. Above the percolation threshold the conductivity increases further toward the value of the aqueous phase and the decrease toward the percolation threshold can also be described by a power law with an exponent $t=1.9\pm0.1$, consistent with the static percolation index [9,10]. The frequency dependence of the dielectric constant has also been measured by us in the dense-microemulsion regime close to the percolation threshold [10]. Frequency dependence of the dielectric constant is found to deviate from the Debye relaxation form which, in the time domain, would correspond to an exponential decay. We were able to fit both the real and imaginary parts of the dielectric constant by the Cole-Cole dispersion law and extract its exponent α and the average relaxation time τ. Again, we found that the average relaxation time τ increases dramatically on approaching the percolation threshold and the exponent α reaches a maximum there too. Rheological properties of the dense microemulsion have also been studied. We measured the static shear viscosity as well as the ultrasound velocity and absorption [13]. A rapid rise of the static shear

viscosity in the dense microemulsion region has been observed. There is also unambiguous evidence of a viscoelastic behavior of dense microemulsions. The absorption data for various volume fractions and temperatures can be reduced to universal plots by scaling both the sound absorbtion and the frequency by the measured shear viscosity. The viscoelastic behavior can be interpreted as coming from the high-frequency tail of the viscoelatic relaxation, describable by a Cole-Cole relaxation formula with unusually small elastic moduli. The shear viscosity measurements of the microemulsions have been extended by Majolino et al. [14] to different volume fractions and temperatures. They observed a steep rise of the relative viscosity (with respect to decane) on approaching the percolation threshold, reaching a well-defined maximum right after. The data are accounted for by these authors considering the dense microemulsion as a colloidal system in which aggregation phenomena takes place. On the basis of a two-fluid model, they identified two different contributions to the viscosity. The first one is connected to the repulsive (hard-sphere) part of the potential while the second one is directly linked to the small but long-ranged attractive potential that directly contributes to the formation of aggregates. This latter contribution becomes important near the percolation threshold.

Another remarkable feature of the three-component microemulsion system is the occurrence of a dynamic slowing down in relaxation time of the droplet density fluctuations on approaching the volume fraction of $\phi_c=0.65$ at $T=23\,°C$, near the percolation threshold. This phenomenon has been detected by dynamic light-scattering experiments [3,4]. The dynamic slowing down is revealed from the examination of the time-dependent droplet density-density correlation function as a function of ϕ. It decays initially exponentially with a first cumulant Γ_c, and gradually evolves into a stretched exponential of the Kohlrausch-Williams-Watts form. A direct measure of the dynamic slowing down can be obtained by plotting the first cumulant Γ_c as a function of the volume fraction at constant temperature. This plot will result in approximately a linear decrease toward zero at the percolation threshold ϕ_p at that given temperature. Variation of the first cumulant as a function of the magnitude of the scattering wave vector q also shows an unusual feature. Far away from the percolation threshold one observes the usual q^2 dependence, indicating the diffusion of an object the dimension of which is smaller than the incoming wavelength, whereas when close to the percolation threshold one observes a q^3 dependence indicating diffusion of an object the size of which is larger than the wavelength of light. This crossover behavior is similar to light scattering near the critical point. Similar experimental results have also been reported by Magazú et al. [5]. A fit of the long-time tail of the density-density correlation function to a stretched exponential function gives the stretched exponent β which decreases to values as small as 0.7, an approaching ϕ_p, and with the average relaxation time which increases to a maximum of a couple of hundred microseconds. Static light-scattering intensity has also been reported by Magazú et al. [5].

Measurements were performed as a function of the scattering angle in the range from 20°–150°. Close to the percolation threshold, these authors observed a strong dissymmetry in the scattered intensity. The forward scattering increases strongly on approaching the percolation threshold from below. This effect was interpreted as formation in the dense microemulsion of transient fractal aggregates of a fractal dimension D close to two. The microemulsion in the vicinity of cloud point curve, namely in the critical regime, has also been extensively studied by different experimental techniques (neutron scattering [2], light scattering [15], and dielectric relaxation [6]). As evident from the percolation line depicted in Fig. 1, the electrical conductivity is extremely sensitive to percolation phenomena all over the phase diagram including the vicinity of the critical point. On the other hand, light scattering is sensitive to fluctuation of the droplet density. It is thus dominated by the critical fluctuations when near the cloud point curve [15]. However, when the volume fraction is above 0.40, which corresponds to the cusp in the phase diagram, both light scattering and electrical conductivity are sensitive to the dynamical percolation of the microemulsion droplets.

In this paper we shall attempt to undertake a unified analysis of static and dynamic light-scattering data below the percolation threshold based on a model which takes into account explicitly the existence of polydispersed fractal clusters in the dense microemulsions. As we stated above, in this regime the clustering of the microemulsion droplets is well described by a picture of dynamic percolation, which is distinct from the geometrical percolation of the static percolation theory. We shall assume that the average size of the fractal clusters increases according to a power law when approaching the percolation threshold. This is the basic physical mechanism for the dynamic slowing down. It is somewhat surprising that this simple theory can quantitatively account for various experimental measurements described above, using the standard power-law indices for the fractal dimension and the polydispersity exponent taken from three-dimensional percolation theory.

II. THEORY OF DYNAMIC LIGHT SCATTERING FROM POLYDISPERSED FRACTAL CLUSTERS

On the basis of previous small-angle neutron-scattering measurements [1,2], we know that the microemulsion droplet is on the average spherical with an average hydrodynamic radius R_1 of 85 Å. The electric field scattered by a single microemulsion droplet labeled j whose size is much smaller than $1/q_{max}$, where $1/q_{max}$ is about 300 Å in a light-scattering experiment, is given by $ae^{i\mathbf{q}\cdot\mathbf{r}_j}$ where a is the scattering amplitude of a droplet, assumed all identical, and $\mathbf{r}_j$ is the positional vector of the center of mass of the droplet with respect to a fixed origin in the sample. Imagine dividing the sample into a collection of clusters each labeled by an index k. Let $\mathbf{r}_j = \boldsymbol{\rho}_{k,j} + \mathbf{x}_k$ where $\mathbf{x}_k$ is the center-of-mass position vector of the cluster k and $\boldsymbol{\rho}_{k,j}$ is the positional vector of the jth droplet in the kth cluster. The exponential phase factor is thus decomposed into two terms and the scattered electric

field due to all particles in the sample can be written as a sum over the clusters

$$E_s(q,t) = \sum_k A_k(q,t)e^{i\mathbf{q}\cdot\mathbf{x}_k(t)} , \qquad (1)$$

where the amplitude $A_k(q,t)$ is the scattered field due to the collection of the particles inside the k cluster and is given by

$$A_k(q,t) = a^2 \sum_{j=1}^k e^{i\mathbf{q}\cdot\boldsymbol{\rho}_{k,j}(t)} . \qquad (2)$$

The scattered-field time correlation function $G(q,t)$ now is given by

$$G(q,t) = \sum_{k,k'} \langle A_k(q,t)A_{k'}(-q,0)e^{i\mathbf{q}\cdot[\mathbf{x}_k(t)-\mathbf{x}_{k'}(0)]} \rangle , \qquad (3)$$

where the angular brackets denote an ensemble average to be taken over all the possible realizations of the system. We assume that on approaching the percolation threshold, the fluctuation of the amplitude $A_k(q,t)$, which corresponds to the internal rearrangement of the cluster, becomes much slower than the characteristic time of the diffusive motion (translational and rotational motion) of the cluster. Specifically, for the system we are studying, the cluster rearrangement time T_R is of the order or longer than 1 ms near the threshold [10]. On the other hand, the first cumulant of the measured time correlation functions is of the order of 10^4 rad/s which corresponds to a relaxation time of 0.1 ms. Thus we can treat the time evolution of the diffusion of the cluster assuming the cluster to be rigid. This physical assumption allows us to decouple the statistical average in $G(q,t)$ into two separate statistical averages

$$G(q,t) = \sum_{k,k'} \langle A_k(q,t)A_{k'}(-q,0) \rangle \langle e^{i\mathbf{q}\cdot[\mathbf{x}_k(t)-\mathbf{x}_{k'}(0)]} \rangle .$$
$$(4)$$

Since the time scale of the fluctuations of the first factor is much slower than the second, we may to a good approximation set

$$G(q,t) = \sum_k \langle A_k(q,0)A_k(-q,0) \rangle \langle e^{i\mathbf{q}\cdot[\mathbf{x}_k(t)-\mathbf{x}_k(0)]} \rangle . \qquad (5)$$

The fact that we can retain only the diagonal term in k is because we can plausibly argue that at $t=0$, the droplet-droplet correlations exist only within a cluster. In fact, we shall use as the real-space pair-correlation function a form which contains an explicit exponential cutoff factor e^{-r/R_k}, where R_k is the radius of gyration of the k cluster. We have then

$$G(q,t) = \sum_k kS_k(q)e^{-D_kq^2t} . \qquad (6)$$

In writing Eq. (6) we have approximated the second factor in Eq. (4) by $e^{-D_kq^2t}$, expressing continuous diffusion of a cluster containing k droplets. We denote by D_k the effective diffusion constant of a cluster. $S_k(q)$ is the intracluster structure factor defined as

$\langle A_k(q,0)A_k(-q,0)\rangle/k$, which we shall introduce explicitly later on. In practice, we can replace the sum over k by an integral over k extending from one to infinity by introducing a cluster size distribution function $N(k)$. We finally obtain the central formula for the intermediate scattering function

$$G(q,t)=\int_1^\infty dk\ N(k)kS_k(q)e^{-D_kq^2t}\ .\qquad(7)$$

In photon correlation spectroscopy one measures the normalized function $C(q,t)=G(q,t)/G(q,0)$. The intraparticle structure factor $S_k(q)$ for a fractal cluster containing k droplets, where q is the Bragg wave number of the scattering, has been given by Chen and Teixeira [16]. In the q range for light scattering, aside from a constant factor, it can be written as

$$S_k(q)=k\frac{\sin[(D-1)\arctan(qR_k)]}{(D-1)qR_k(1+q^2R_k^2)^{(D-1)/2}}\ .\qquad(8)$$

This is the Fourier transform of a pair-correlation function $g(r)=r^{D-3}\exp(-r/R_k)$. In Eq. (8), R_k is the radius of gyration of the k cluster and D its fractal dimension, the two being connected by the relation $R_k=R_1k^{1/D}$. In the light-scattering range $qR_1\approx0.1$ so the droplet form factor is always nearly unity. From Eq. (8), for $qR_k<1$, $S(k,q)$ can be approximated as

$$S_1(k,q)\approx k[1-\tfrac{1}{6}D(D-1)q^2R_k^2]$$

$$\approx k\exp\{-[D(D+1)/6]q^2R_k^2\}$$

while for $qR_k>1$, it takes the form

$$S_2(k,q)\approx k\{\sin[(D-1)\pi/2]/(D-1)\}(qR_k)^{-D}\ .$$

The cluster-size distribution function $N(k)$ for the percolation clusters has the scaling form [17] $N(k)=k^{-\tau}f(k^\sigma/s^\sigma)$, characterized by the two exponents τ and σ, and where s has the meaning of average number of droplets in a cluster. Numerical simulations for three-dimensional percolation clusters indicated a fractal dimension of $D=2.5$, a polydispersity exponent $\tau=2.2$, and $\sigma=0.45$ [17]. Assuming $\sigma\approx0.5$ and a Gaussian cutoff function [18,19], we have $N(k)\approx k^{-\tau}e^{-k/s}$.

The scattered intensity is assumed to follow the Ornstein-Zernike law, as suggested by experiment [5], which, when normalized by its $q=0$ value I_0, can be written as

$$\frac{I(x)}{I_0}=(1+x^2)^{-1}\ ,\qquad(9)$$

where we have introduced the correlation length ξ and the scaled variable $x=q\xi$. The behavior of the normalized intensity is reported in Fig. 2, together with the experimental points measured by Magazú et al. [5] at 25 °C and volume fractions of the dispersed phase ranging from 0.05 to 0.58. The parameters we used to make the comparison between the theory and the experiment are the ones pertinent to percolation, namely $D=2.5$ and $\tau=2.2$, together with the value of the exponent $\nu=0.88$ which determines the divergence of the correlation length on
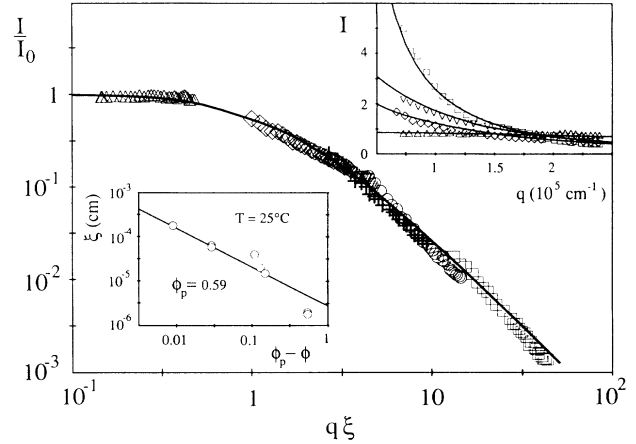

FIG. 2. The normalized scattered intensity as a function of the scaled variable $x=q\xi$ for the set of data reported in Ref. [5], approaching the percolation threshold at constant temperature. The inset shows the measured data.

approaching the percolation point $\xi=\xi_0(\phi_p-\phi)^{-\nu}$. We get $\phi_p=0.59$, in accordance with the measured value on the percolation line [6], and $\xi_0=257$ Å, a value of the order of magnitude of the constituent droplet diameter $2R_1$.

The calculation of the scattering properties from a polydisperse system proceeds along the line similar to the one used by Martin and co-workers [20,19,21,22] for percolation clusters and colloidal aggregates. If we assume that the clusters are rigid, the first cumulant

$$\Gamma_c=-\left[\frac{1}{C(t)}\frac{dC(t)}{dt}\right]_{t=0}$$

of the normalized droplet density-time correlation function $C(t)$ can be calculated as

$$\Gamma_c(x)=\frac{1}{G(q,0)}\int_1^\infty dk\ N(k)k^2S_k(q)D_k^{\text{eff}}q^2\ ,\qquad(10)$$

where $D_k^{\text{eff}}\approx D_k(1+1/2\rho^2)$ is the effective diffusion coefficient and $D_k=D_1k^{-1/D}$ is the translational diffusion coefficient of the k cluster. The effective diffusion coefficient includes both the translational and the rotational motion of the cluster. The latter is written in terms of the translational diffusion coefficient, a derivative of the interparticle correlation function and the ratio ρ of the hydrodynamic radius to the radius of gyration of the k cluster D_k, a quantity that we assume to be of the order of one [23]. The result for the dimensionless linewidth $\Gamma_c^*=\Gamma_c/D_1R_1q^3$ is

$$\Gamma_c^*(x)=\frac{F(3-\tau-1/D,x)}{G(x,0)}(1+x^2)^{-(D/2)(3-\tau-1/D)}$$

$$+\left[1+\frac{1}{2\rho^2}\right]\frac{H(2-\tau-1/D,x)}{G(x,0)}\left[\frac{x}{h}\right]^{-D}\qquad(11)$$

with

$$G(x,0)=F(3-\tau,x)(1+x^2)^{-(D/2)(3-\tau)}$$

$$+H(2-\tau,x)(x/h)^{-D} . \tag{12}$$

We have defined the two scaling functions dominant in the small and large x range as

$$F(a,x)=\Gamma(a)-\Gamma(a,h^2(1+x^2)/x^2)$$

and

$$H(a,x)=\{\sin[(D-1)\pi/2]/(D-1)\}\Gamma(a,(x/h)^{-D}) ,$$

where $\Gamma(a,x)=\int_x^\infty dt\, t^{a-1}e^{-t}$ is the incomplete gamma function and $h=[D(D+1)/6]^{1/2}$. The dimensionless linewidth shows the behavior $\Gamma_c^*\approx x^{-1}$ for $x\ll 1$ and $\Gamma_c^*\approx$ const for $x\gg 1$, when $\tau>2$. To support the model, we have performed a series of dynamic light-scattering experiments in the dense one-phase region of the decane–water–AOT microemulsion system, corresponding to $X=40.8$, in the vicinity of the volume fraction ϕ equal to 0.60. We have also analyzed the published data of Chen and Huang [3], Sheu et al. [4], and Magazú et al. [5]. Figure 3 shows the scaled first cumulant Γ_c^* plotted as a function of x^{-1}. Data are taken from a set of measurements performed by Chen and Huang [3], Sheu et al. [4], Magazú et al. [5], and ourselves and fall essentially in the region $0.5<x<10$. The experimental data indicate a crossover from a q^2 to a q^3 dependence of the cumulant near $q\xi=1$. It is to be noted that we use the same value of the parameter ξ_0 for all the measurements.

FIG. 3. The scaled linewidth for short times as a function of the scaled variable x^{-1}. Data are taken from the references quoted. The inset shows the measured data.

However, we change ϕ_p for different temperatures, according to the measured percolation locus [6]. The inset shows the measured cumulant as a function of ϕ at constant q, and illustrates again the collapse of the measurements according to the predicted universal law. Finally, we compute the full density-density time correlation function in order to study its long-time behavior. Using the method described above, we obtain

$$C(x,v)=\frac{(1+x^2)^{-(D/2)(3-\tau)}}{G(x,0)}\int_0^{[h^2(1+x^2)/x^2]^{D/2}} dz\, z^{2-\tau}\exp[-z-v(1+x^2)^{1/2}z^{-1/d}]$$

$$+\frac{\sin[(D-1)\pi/2]}{(D-1)}\frac{(x/h)^{-D}}{G(x,0)}\int_{(x/h)^{-D}}^\infty dz\, z^{1-\tau}e^{-z-vz^{-1/d}} \tag{13}$$

with $v=D_1q^2t/s^{1/D}=D_1R_1hq^2t/\xi$. The integrals can be evaluated numerically for all times. Figure 4 shows typical fits to a set of data taken at different volume fractions and corresponding to the values $x\approx 1$, 3.5, and 17. It is interesting to note that for very long times, where the

method of steepest descent can be applied, the leading terms of the two integrals in Eq. (13) are
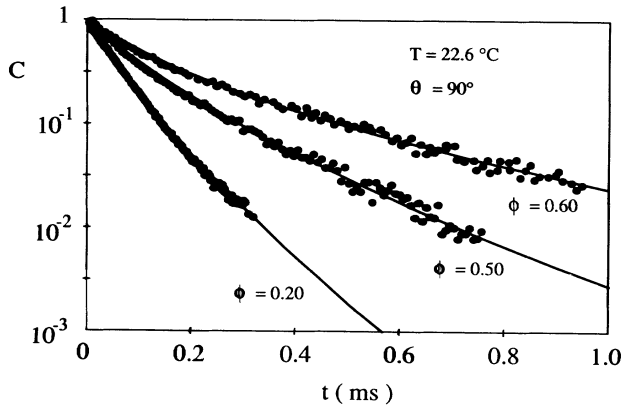
$$\exp\{-(D+1)[v(1+x^2)1/2/Dx]^\beta\}$$

FIG. 4. Typical normalized time correlation function for various volume fractions, from Ref. [3]. The solid lines are given by the present theory and are indistinguishable from a stretched exponential.
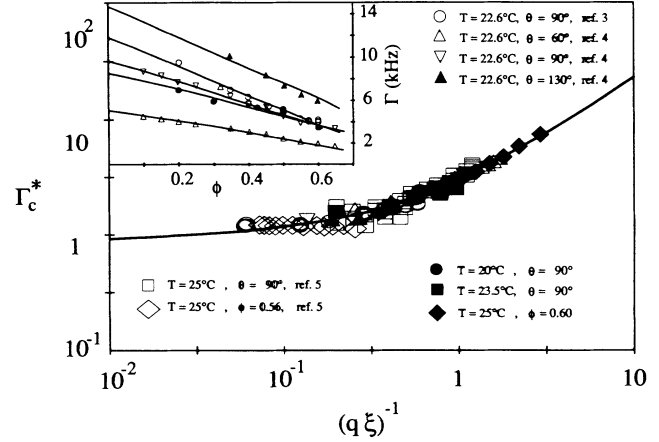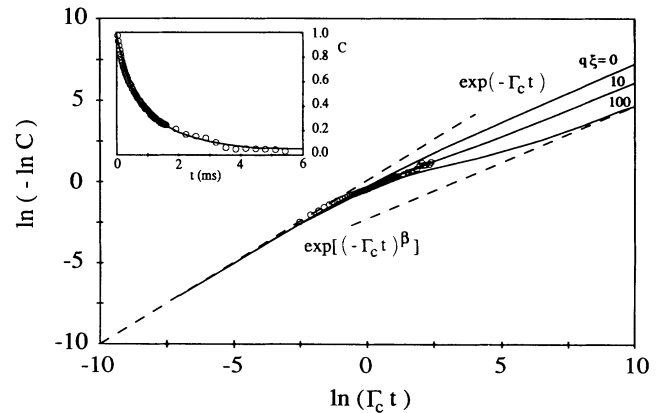
FIG. 5. The normalized time correlation function for various values of x, in terms of the dimensionless variable $\Gamma_c t$. The dashed lines indicate the limiting slopes $\beta=1$ and $\beta=D/(D+1)$ for short and long times, respectively. The inset shows the measured correlation function.

and

$$\exp[-(D+1)(v/D)^{\beta}] \, ,$$

respectively, with $\beta=D/(D+1)$. We can use the dimensionless quantity $\Gamma_c t = \Gamma_c^*(x/h)v$ in order to eliminate the scaling parameter v and construct a plot of the correlation function C as a function of the dimensionless variable $\Gamma_c t$. The plot of Fig. 5 shows that the correlation function decays initially exponentially like $\exp(-\Gamma_c t)$ and gradually evolves into a stretched exponential $\exp[-(\Gamma_s T)^{\beta}]$ with $\Gamma_s \approx q^2$. The experimental data cover the range up to $\ln(\Gamma_c t)\approx 2$.

III. CONCLUSIONS

In summary, based on an approximate scattering theory applied to a collection of polydisperse fractal percolation clusters, we were able to explain quantitatively the dynamic slowing-down phenomena observed near the volume fraction 0.6, previously attributed to a glasslike transition [3,4]. We have been able to document unambiguous evidence of percolation occurring at $\phi=0.6$ at $T=23\,°C$. The first cumulant Γ_c of the droplet density correlation function can be set in a scaled form in the variable $x=q\xi$, as given in Eq. (11). The complete analytical form of the correlation function is given in Eq. (12), which asymptotically approaches a stretched exponential form for times much longer than $150/\Gamma_c$ (see Fig. 5). Although the true stretched exponent in the theory is a universal number, $\beta=D/(D+1)$, the apparent stretched exponent β^*, observed in previous experiments [3,4], can vary anywhere between 0.6 and 1, because the time correlation functions used in the fitting extend only to the transition range $t \approx 1/\Gamma_c$ in the universal plot given in Fig. 5. Furthermore, since Γ_c is a function of $q\xi$, the apparent exponent β^* is also a function of q and ϕ. Likewise, as one approaches the percolation threshold, the transition region moves up to longer times and thus the measured β^* approaches unity. In order to measure the true exponent β and hence the fractal dimension D, one needs to measure the correlation function in the range from 1 ms to 1 s.

It is pertinent to remark here that the theory presented above near the percolation threshold bears a striking resemblance to the well-known static and dynamic fluctuations theory near the critical point [19,24]. Both theories share a common feature, that the scaled intensity and linewidth can be expressed in terms of universal functions of the single scaling variable x. However, we wish to stress that the phenomenon of dynamic slowing down we observed near the volume fraction of 0.6 is distinct from the critical phenomenon occurring near the cloud point curve at low volume fractions, where we have previously made an extensive light-scattering investigation [15].

[1] M. Kotlarchyk, S. H. Chen. J. S. Huang, and M. W. Kim, Phys. Rev. Lett. **53**, 941 (1984).

[2] M. Kotlarchyk, S. H. Chen, J. S. Huang, and M. W. Kim, Phys. Rev. A **28**, 508 (1983); **29**, 2054 (1984).

[3] S. H. Chen and J. S. Huang, Phys. Rev. Lett. **55**, 1888 (1985).

[4] E. Y. Sheu, S. H. Chen, J. S. Huang, and J. C. Sung, Phys. Rev. A **39**, 5867 (1989).

[5] S. Magazú, D. Majolino, G. Maisano, F. Mallamace, and N. Micali, Phys. Rev. A **40**, 2643 (1989).

[6] C. Cametti, P. Codastefano, P. Tartaglia, J. Rouch, and S. H. Chen, Phys. Rev. Lett. **64**, 1461 (1990).

[7] H. F. Eicke, M. Borkovec, and B. Das-Gupta, J. Phys. Chem. **93**, 314 (1989).

[8] D. G. Hall, J. Phys. Chem. **94**, 429 (1990).

[9] G. S. Grest, I. Webman, S. A. Safran, and A. L. R. Bug, Phys. Rev. A **33**, 2842 (1986).

[10] C. Cametti, P. Codastefano, A. Di Biasio, P. Tartaglia, and S. H. Chen, Phys. Rev. A **40**, 1962 (1989).

[11] J. Xu and G. Stell, J. Chem. Phys. **89**, 1101 (1988); G. Stell, J. Phys. A **17**, L855 (1984).

[12] S. H. Chen, T. L. Lin, and M. Kotlarchyk, in *Surfactant in Solutions*, edited by P. Bothorel and K. Mittal (Plenum, New York, 1987), Vol. II; S. H. Chen, T. L. Lin, and J. S. Huang, in *Physics of Complex and Supramolecular Fluids*, edited by S. A. Safran and N. A. Clark (Wiley, New York, 1987).

[13] C. Cametti, P. Codastefano, G. D'Arrigo, P. Tartaglia, J. Rouch, and S. H. Chen, Phys. Rev. A **42**, 3421 (1990).

[14] D. Majolino, F. Mallamace, S. Venuto, and N. Micali, Phys. Rev. A **42**, 7330 (1990).

[15] J. Rouch, A. Safouane, P. Tartaglia, and S. H. Chen, J. Chem. Phys. **90**, 3756 (1989).

[16] S. H. Chen and J. Teixeira, Phys. Rev. Lett. **57**, 2583 (1986).

[17] D. Stauffer, Phys. Rep. **54**, 1 (1979).

[18] P. L. Leath, Phys. Rev. Lett. **36**, 921 (1976); Phys. Rev. B **14**, 5046 (1976).

[19] J. E. Martin and B. J. Ackerson, Phys. Rev. A **31**, 1180 (1985).

[20] J. E. Martin and D. W. Schaefer, Phys. Rev. Lett. **53**, 2457 (1984).

[21] J. E. Martin and F. Leyvraz, Phys. Rev. A **34**, 2346 (1986).

[22] J. E. Martin, Phys. Rev. A **36**, 3415 (1987).

[23] M. Y. Lin, H. M. Lindsay, D. A. Weitz, R. C. Ball, R. Klein, and P. Meakin, Proc. R. Soc. London Ser. A **423**, 71 (1989).

[24] K. Kawasaki, Ann. Phys. (N.Y.) **61**, 1 (1970).